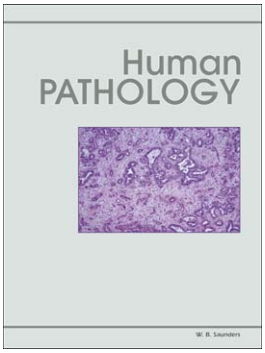

Distribution and components of interstitial inflammation and fibrosis in IgG4-related kidney disease: Analysis of autopsy specimens

Satoshi Hara MD, Mitsuhiro Kawano MD, PhD, Ichiro Mizushima MD, PhD, Kenichi Harada MD, PhD, Takuma Takata MD, PhD, Takako Saeki MD, PhD, Yoshifumi Ubara MD, PhD, Yasuharu Sato MD, PhD, Michio Nagata MD, PhD

PII: S0046-8177(16)30091-0
DOI: doi: 10.1016/j.humpath.2016.05.010
Reference: YHUPA 3908

To appear in: *Human Pathology*

Received date: 15 December 2015
Revised date: 30 March 2016
Accepted date: 19 May 2016

Please cite this article as: Hara Satoshi, Kawano Mitsuhiro, Mizushima Ichiro, Harada Kenichi, Takata Takuma, Saeki Takako, Ubara Yoshifumi, Sato Yasuharu, Nagata Michio, Distribution and components of interstitial inflammation and fibrosis in IgG4-related kidney disease: Analysis of autopsy specimens, *Human Pathology* (2016), doi: 10.1016/j.humpath.2016.05.010

Original Contribution

Distribution and components of interstitial inflammation and fibrosis in IgG4-related kidney disease: Analysis of autopsy specimens

Satoshi Hara, MD[1,2], Mitsuhiro Kawano, MD, PhD[2], Ichiro Mizushima, MD, PhD[2], Kenichi Harada, MD, PhD[3], Takuma Takata, MD, PhD[4], Takako Saeki, MD, PhD[5], Yoshifumi Ubara, MD, PhD[6], Yasuharu Sato, MD, PhD[7], and Michio Nagata, MD, PhD[1].

[1]Department of Kidney and Vascular Pathology, University of Tsukuba, Tsukuba, 305-8575 Japan

[2]Division of Rheumatology, Department of Internal Medicine, Kanazawa University Graduate School of Medicine, Kanazawa, 920-8641 Japan

[3]Department of Human Pathology, Kanazawa University Graduate School of Medicine, Kanazawa, 920-8640 Japan

[4]Department of Internal Medicine, Nagaoka Chuo General Hospital, Nagaoka, 940-8653 Japan

[5]Department of Internal Medicine, Nagaoka Red Cross Hospital, Nagaoka, 940-2108

Japan

[6]Nephrology Center, Toranomon Hospital, Kajigaya, 213-8587 Japan

[7]Department of Pathology, Okayama University Graduate School of Medicine, Dentistry and Pharmaceutical Sciences, Okayama, 700-8558 Japan

Corresponding author: Mitsuhiro Kawano.

Division of Rheumatology, Department of Internal Medicine, Kanazawa University Graduate School of Medicine, Kanazawa, Japan.

Address: 13-1 Takara-machi, Kanazawa, Ishikawa, 920-8641 Japan.

Tel: +81-76-265-2253, Fax: +81-76-234-4251

E-mail: sk33166@gmail.com

Keywords: IgG4-related kidney disease, IgG4-related disease, interstitial fibrosis, storiform fibrosis, bird's-eye pattern fibrosis

Running head: Autopsy analysis of IgG4-related kidney disease

Conflicts of Interest: The authors have no conflicts of interest related to this study.

Funding Disclosure: This work was supported by Health and Labour Sciences Research Grants for the Study of Intractable Diseases from the Ministry of Health, Labour and Welfare, Japan.

Abstract

IgG4-related kidney disease (IgG4-RKD) occasionally progresses to chronic renal failure and is pathologically characterized by IgG4-positive lymphoplasmacyte-rich tubulointerstitial nephritis with storiform fibrosis (bird's-eye pattern fibrosis). Although radiology reveals a heterogeneous distribution of affected areas in this disease, their true distribution within the whole kidney is still unknown because of difficulty in estimating this from needle biopsy samples.

Using 5 autopsy specimens, the present study histologically characterized the distribution and components of interstitial inflammation and fibrosis in IgG4-RKD. Interstitial lymphoplasmacytic infiltration or fibrosis was observed in a variety of anatomical locations such as intracapsular, subcapsular, cortical, perivascular, and perineural regions heterogeneously in a patchy distribution. They tended to be more markedly accumulated around medium- and small-sized vessels. Storiform fibrosis was limited to the cortex. Immunostaining revealed nonfibrillar collagens (collagen IV and VI) and fibronectin predominance in the cortical lesion, including storiform fibrosis. In contrast, fibril-forming collagens (collagen I and III), collagen VI and fibronectin were the main components in the perivascular lesion. In addition, alpha-smooth muscle actin-positive myofibroblasts were prominently accumulated in the early lesion and

decreased with progression, suggesting that myofibroblasts produce extracellular matrices forming a peculiar fibrosis.

In conclusion, perivascular inflammation or fibrosis of medium- and small-sized vessels is a newly identified pathological feature of IgG4-RKD. Because storiform fibrosis contains mainly nonfibrillar collagens, "interstitial fibrosclerosis" would be a suitable term to reflect this. The relation between the location and components of fibrosis determined in whole kidney samples provides new clues to the pathophysiology underlying IgG4-RKD.

Keywords: IgG4-related kidney disease, IgG4-related disease, interstitial fibrosis, storiform fibrosis, bird's-eye pattern fibrosis

1. Introduction

IgG4-related kidney disease (IgG4-RKD) is a major manifestation of IgG4-related disease (IgG4-RD) [1,2]. The typical histology, IgG4-positive plasma cell (PC)-rich tubulointerstitial nephritis (TIN), occasionally progresses to chronic renal failure [3,4].

One basic pathological feature of IgG4-RKD is a curious distribution of its inflammation. Radiologically, the lesions distribute heterogeneously within the kidney such as capsule, cortex, medulla, and renal pelvis [1]. Reflecting the radiological findings, histology shows its specific features: a clear demarcation between lesions and non-lesions, and extension of a lesion often beyond the renal capsule [3,5]. However, it remains unknown how IgG4-positive PCs infiltrate heterogeneously in the kidney structures because of the insufficient size of tissue specimens obtainable by needle biopsy. In this regard, autopsy specimens are ideal for analyzing the distribution of inflammation and fibrosis.

In addition to location, the interstitial fibrosis, called ‘storiform fibrosis’ or ‘bird’s-eye pattern fibrosis’, is another important disease-specific histological hallmark of IgG4-RKD that clearly distinguishes IgG4-related from non-IgG4-related TIN [3,5]. Electron microscopic analysis suggests that storiform fibrosis contains more extracellular matrix (ECM) components than fibrous materials [3]. Thus, this peculiar

fibrosis may consist of different ECM proteins from other stages of fibrosis in IgG4-RKD and non-IgG4-related TIN. However, it remains undetermined whether different stages of interstitial lesions, including storiform fibrosis, contain the same ECM proteins.

In the present study, we histologically identified the characteristic distribution of interstitial inflammation and fibrosis in IgG4-RKD, using autopsy kidneys. Subsequently, we analyzed and compared the characteristic components of interstitial fibrosis according to the locations by immunostaining. Our findings may facilitate better understanding of the pathophysiology of IgG4-RKD.

2. Materials and Methods

2.1. Subjects

Five autopsy derived whole kidneys from IgG4-RKD patients were enrolled (Kanazawa University, Nagaoka Red Cross Hospital, Nagaoka Chuo General Hospital, Toranomon Hospital and Okayama University). The diagnoses of IgG4-RKD and IgG4-RD were made according to established diagnostic criteria [2,4,6]. Serum samples were also obtained at the time of diagnosis of IgG4-RD. Cases 3 and 4 were described in previous reports [7,8]. Biopsied kidney specimens from idiopathic TIN (n = 3),

diabetic nephropathy (n = 2), and benign nephrosclerosis (n = 2) were used to compare ECM proteins with those of IgG4-related TIN. The study was approved by the ethics committee of Kanazawa University (No. 2013-833).

2.2. Histochemical and immunohistochemical analyses

Autopsies were performed 2.2, 1.5, 8, 1.5, and 8 h after death in cases 1 to 5, respectively. All samples were fixed in formaldehyde and embedded in paraffin blocks, and were used for hematoxylin and eosin, periodic acid-Schiff, periodic acid methenamine silver (PAM), Masson's Trichrome (MT) staining, and immunostaining. Specific primary antibodies for immunostaining were as follows: monoclonal mouse anti-human IgG4 antibody (clone HP6025; ready-to-use; Nichirei Bioscience, Tokyo, Japan), monoclonal mouse anti-human CD138 antibody (clone B-A38; 1:100; AbD Serotec, Oxford, UK), monoclonal mouse anti-human collagen I antibody (clone COL-1; 1:100; Abcam, Cambridge, UK), polyclonal rabbit anti-human collagen III antibody (1:400; Abcam), polyclonal rabbit anti-human collagen IV antibody (1:200; Abcam), monoclonal mouse anti-human collagen V antibody (clone 1E2-E4/Col5; 1:50; Abcam), polyclonal rabbit anti-human collagen VI antibody (1:100; Abcam), polyclonal rabbit anti-human fibronectin antibody (1:2,000; Dako, Glostrup, Denmark), and

monoclonal mouse anti-human alpha-smooth muscle actin (α-SMA) antibody (clone 1A4; 1:400; Sigma-Aldrich, MO, USA). For immunostaining, antigen was retrieved by a microwave (10 mM citrate buffer; pH 6.0) for IgG4, CD138, collagen I, fibronectin and α-SMA, or 100 μg/mL of proteinase K (Wako Pure Chemical Industries, Osaka, Japan) for collagen III, IV, V and VI. Thereafter, primary antibodies of rabbit origin were incubated in EnVision labeled polymer-horseradish peroxidase (Dako), and primary antibodies of mouse origin were incubated in a Histofine kit (Nichirei Bioscience) followed by reaction with peroxidase-conjugated streptavidin (Nichirei Bioscience). Peroxidase activity was visualized using a liquid diaminobenzidine substrate (Dako). Hematoxylin was used to stain nuclei.

Interstitial inflammation was classified according to the stage and location. Stages were defined as: stage A, acute interstitial nephritis pattern with minimal interstitial fibrosis; stage B, active cellular infiltration with mild but distinct expansile interstitial fibrosis; stage C, interstitial fibrosis dominant with mild cellular infiltration; stage D, advanced interstitial fibrosis with less cellular infiltration [3,4]. Storiform fibrosis or bird's-eye pattern fibrosis is defined as an irregular pattern of fibrosis resembling the spokes of a cartwheel with infiltrating cells radiating from the center [3,9]. Locations were divided into intracapsule, subcapsule, cortex (except for subcapsular, perivascular

and perineural lesions), perivasculature, perinerve and medulla.

For comparison of different staining at the same location, we obtained synchronized images using Nano-Zoomer 2.1S (Hamamatsu Photonics, Hamamatsu, Japan).

2.3. Statistics

All data are presented as absolute numbers or means ± standard errors. Statistical differences between two or more than three groups were evaluated using unpaired Student *t* test and Welch's test, respectively. $p < 0.05$ was deemed to indicate statistical significance.

3. Results

3.1. Clinical profiles

The patients were all Japanese males with an average age of 71.2 ± 2.2 (range 64-76) years at the time of diagnosis of IgG4-RD (**Table 1**). The mean intervals from diagnosis to death were 63.2 ± 15.5 (range 1-108) months. All patients demonstrated serum IgG and IgG4 elevations (IgG mean 3,886 mg/dL, range 2,430-4,813 mg/dL; IgG4 mean 1,284 mg/dL, range 319-1,750 mg/dL). Four of the 5 cases (80%) had hypocomplementemia, and all had extra-renal involvement, including pancreas, salivary

gland, lung, liver, bile duct, aorta, retroperitoneum, lymph nodes, prostate gland, and skin. Two patients (40%; cases 1 and 2) were receiving prednisolone at the time of death. The other 2 patients (cases 4 and 5) were receiving chemotherapy for malignancy. The causes of death were sepsis in 2 cases and sudden death of unknown cause, nonocclusive mesenteric ischemia and recurrence of a mucinous cystadenocarcinoma of the appendix with peritoneal dissemination in one each of the remaining 3 cases.

3.2. Histopathological features

Microscopically, all cases showed dense interstitial lymphoplasmacytic infiltration and/or fibrosis **(Table 2)**. In 2 of 5 specimens without corticosteroid (cases 3 and 5), storiform fibrosis was present (**Fig. 1A**). Obliterative phlebitis or lymphoid follicles were absent in all cases. Lymphoplasmacyte infiltration or fibrosis was detected around interlobar, arcuate or interlobular artery segments (width 200-500 μm) or veins in all cases (**Table 2 and Fig. 1C-F**). Two patients who had received long-term corticosteroid therapy (cases 1 and 2) showed mild and patchy infiltration of lymphoplasmacytes and mild phlebitis, but had a large fibrotic area lacking tubules with few remnant glomeruli and arteries **(Fig. 1, G and H)**.

With respect to location, interstitial inflammation was noted in the intracapsule in 2,

subcapsule in 3, cortex and perivasculature in 5, perinerve in one, but in the medulla in none (**Table 3**). Lymphoplasmacytic infiltration or fibrosis was located mainly in the cortex and perivasculature. Of note is that each specimen contained a variety of stages of inflammation in different locations and that storiform fibrosis was limited to the cortex.

By immunohistochemistry, a marked infiltration of IgG4-positive cells was demonstrated in the tubulointerstitium (mean IgG4 counts, 63.4; range, 3.4-116/high power field [HPF]; **Table 2 and Fig. 1B**) and the IgG4/CD138 ratio was increased (mean IgG4/CD138 ratio, 68.2%; range 14-110%). From these data, 4 of 5 patients (cases 1, 3-5) satisfied diagnostic criteria for IgG4-RD and IgG4-RKD, and the consensus statement on the pathology of IgG4-RD [2,4,6,9]. The remaining one who had received long-term corticosteroid (case 2) showed little lymphoplasmacytic infiltration at autopsy (IgG4-positive cell count, 3.4/HPF; IgG4/CD138 ratio, 14%), but numerous IgG4-positive PCs infiltrated the tubulointerstitium in the kidney biopsy specimen.

3.3. Location and stage dependent components of interstitial fibrosis

According to the location and stage, we investigated characteristic features of

IgG4-RKD using standard staining and immunohistochemistry (**Fig. 2, 3 and Table 4**).

Intracapsular lesions showed stages A and D without storiform fibrosis. At stage D, PAM-positive and MT-blue apparent fibers were predominant, and were stained by collagen I and fibronectin. Subcapsular lesions showed stages B and D without storiform fibrosis. In these lesions, fibrosis was PAM-negative and was stained by fibronectin. Cortical lesions revealed all stages including storiform fibrosis. Thin fibers were apparent at stage B and subsequently formed thick fibers and encircled infiltrating lymphoplasmacytes at stage C (storiform fibrosis), and finally a fiber-rich lesion formed stage D. The fibers were PAM-positive and MT-blue, and were stained by collagen IV, VI and fibronectin predominantly, but less with collagen I and III. Perivascular lesions showed stages A, B, and D, but no storiform fibrosis. Thin fibers similar to those in the cortical lesions appeared at stage B. At stage D, biphasic fibers were predominant components showing PAM-negative MT-weak blue and PAM-positive MT-strong blue pictures. The former fibers consisted of collagen VI and fibronectin, and collagen I and III were added to the latter. Perineural lesions showed only stage B. PAM-positive and MT-blue fibers appeared that is stained with collagen I and III. No specimens contained collagen V in any locations or stages.

To compare the ECM components between IgG4-RKD and non-IgG4-related TIN, we

also performed immunostaining in kidney needle biopsy specimens of non-IgG4-related TIN, including idiopathic TIN, diabetic nephropathy, and benign nephrosclerosis **(Suppl Fig.)**. In the cortex, interstitial fibrosis tended to contain more collagen I than collagen III, IV, VI and fibronectin. The components did not differ between the etiologies of non-IgG4-related TIN.

3.4. Decrease of myofibroblasts with advancing stage

We investigated interstitial α-SMA-positive cell infiltration according to the location and stage. The number of α-SMA-positive cells did not differ at the same stage in any of the locations. With regard to the stage, the number of α-SMA-positive cells was significantly higher in stage A and B, and decreased with advancing stage (stage A, 72.4 ± 12.3; stage B, 50.3 ± 6.4; stage C, 31.4 ± 6.1; stage D; 12.6 ± 4.6/HPF; **Fig. 4)**.

4. Discussion and Conclusions

In the present study, analysis of autopsy specimens clarified characteristic locational features of inflammation and fibrosis in IgG4-RKD. Light microscopy revealed that interstitial inflammation or fibrosis was located mainly in the cortical and perivascular area of medium- and small-sized vessels. The perivascular distribution resembles that of

IgG4-related periaortitis which shows IgG4-positive PC infiltration in the aortic adventitia [10,11]. In addition to aortic lesions, IgG4-RD can also affect coronary artery, forming as a periarteritis [12,13]. These similarities of perivascular lesions suggest that lymphoplasmacytic infiltration extends along the adventitia of large-, medium-, and then small-sized arteries, forming a heterogeneous distribution in the involved organs including kidney in IgG4-RD. Since few reports have focused on the presence or absence of periarterial lesions in individual affected organs such as pancreas, further studies are needed to evaluate the significance of periarterial lesions in IgG4-RD. In addition, further studies using animal models are needed to confirm or refute the hypothesis that perivascular inflammation underlies the pathophysiology of IgG4-RKD.

Another finding in our study is that mixed stages are present in the same kidney in different locations. Histology contained areas of active inflammation with background interstitial fibrosis, even after the achievement of remission by corticosteroid therapy. These findings are important, because clinically inactive but histologically active inflammation may result in extension of interstitial fibrosis and renal dysfunction.

Storiform fibrosis (bird's-eye pattern fibrosis) is a characteristic pathological feature of IgG4-RKD; however, its localization and accumulated protein are unknown. We found that it was formed only in the cortical lesions and the component was predominantly

nonfibrillar ECM proteins. Collagen, a representative ECM protein, is classified as fibril-forming, network-forming, beaded-filament-forming, and other collagens by their function and domain homologies [14]. Immunostaining analysis in the present study revealed that the cortical lesions, including storiform fibrosis, contained mainly network-forming (collagen IV) and beaded-filament-forming collagens (collagen VI), while the perivascular lesions contained fibril-forming collagens (collagen I and III). In contrast, renal fibrosis in non-IgG4-related TIN consists mainly of fibril-forming collagens (collagen I and III) in our study and confirmed previous reports [15,16]. Thus, the cortical lesions in IgG4-RKD have different components from those of non-IgG4-RD-derived renal fibrosis. In addition, a previous electron microscopic study showed that storiform fibrosis contained low-dense matrix components in addition to interstitial-type collagen fibrils [3], supporting our immunohistochemical findings. Thus, storiform fibrosis would be specific in the point of nonfibrillar collagen predominance, compared to interstitial fibrosis of non-IgG4-related TIN which has fibril-forming collagen predominance. We would like to propose that the character of storiform fibrosis could be described as ‘fibrosclerosis’ or ‘sclerosing fibrosis’ to emphasize the ECM-rich composition in addition to fibrous components in IgG4-RKD.

Our next interest is the difference in interstitial components between the cortical and

perivascular lesions of IgG4-RKD. We identified α-SMA-positive cells, a typical marker of myofibroblasts [15], among lymphoplasmacytes in the early phase, which decreased in parallel with advancing stage. Electron microscopy also revealed myofibroblasts among lymphoplasmacyte infiltrates in the early phase [3]. The number of tissue α-SMA-positive cells and amount of collagen accumulation are correlated with the disease activity of IgG4-RD [17]. Myofibroblasts produce collagen IV and fibronectin in addition to collagen I and III [18,19]. These findings suggest that myofibroblasts are a major source of ECMs in IgG4-RD. Furthermore, a variety of studies using rodent models have indicated that myofibroblasts have multiple origins such as resident fibroblasts, bone marrow derived fibroblasts, pericytes, epithelial-mesenchymal transition from tubular cells, and endothelial-mesenchymal transition [20,21]. These different origins of myofibroblasts may associate with the production of different ECMs according to the locations even in the same profibrotic cytokine environment including transforming growth factor-beta (TGF-β), which is speculated to be the main cytokine for organ fibrogenesis in IgG4-RKD [16,22]. In the analyses of fibrosis in other involved organs of IgG4-RD, some new findings were clarified. One group found that epithelial-mesenchymal transition may associate with fibrosis in the lacrimal gland involvement of IgG4-RD [23]. Some other groups recently

showed in studies on IgG4-related sialadenitis that M2-type macrophages and mast cells are other contributors to organ fibrogenesis [24-26]; however, it remains undetermined whether these cells and epithelial-mesenchymal transition contribute to the fibrogenesis of IgG4-RKD. Our data are limited to IgG4-RKD, precluding any conclusion as to whether storiform fibrosis in other organs involved by IgG4-RD contain characteristic ECM components.

Cytokine environment would determine the type of ECMs produced by myofibroblasts, forming characteristic interstitial fibrosis in IgG4-RKD. The major cytokine is TGF-β which is secreted by regulatory T (Treg) cells [27,28]. In IgG4-RKD, quantitative RT-PCR and immunostaining studies have shown that TGF-β mRNA was overexpressed in the biopsy specimens of IgG4-RKD and that Treg cells expressed TGF-β in the interstitium and the number of Treg cells was correlated with IgG4-positive PCs infiltration [16,22]. These findings suggest that Treg-mediated TGF-β affects fibrogenesis in IgG4-RKD. TGF-β is not specific for IgG4-RKD because this cytokine is also expressed in many chronic kidney diseases as a common pathway for progression of interstitial fibrosis [15]. Therefore, our finding, namely that storiform fibrosis has characteristic ECMs, suggests that another specific cytokine may also contribute to the fibrogenesis in IgG4-RKD.

In conclusion, autopsy specimens indicated that perivascular lymphoplasmacytic infiltration or fibrosis of medium- and small-sized vessels would characterize the distribution and pathophysiology of IgG4-RKD. Since our findings showed a predominant component of nonfibrillar collagens as storiform fibrosis, we suggest that this lesion be referred to as fibrosclerosis. Our findings may provide further insight into the pathogenesis of IgG4-RKD.

Acknowledgments

This work was supported by Health and Labour Science Research grants for the Study of Intractable Diseases from the Ministry of Health, Labour and Welfare, Japan. We thank the IgG4-RKD research group of Japan Nephrology Society (Takao Saito, Shinichi Nishi, Hitoshi Nakashima, Satoshi Hisano, Yutaka Yamaguchi, Nobuaki Yamanaka, Motoko Yanagita) for kind advice. We also thank John Gelblum for reading our manuscript.

REFERENCES

[1] Saeki T, Kawano M. IgG4-related kidney disease. Kidney Int 2014;85:251-7.

[2] Kawano M, Saeki T, Nakashima H, Nishi S, Yamaguchi Y, Hisano S, et al. Proposal for diagnostic criteria for IgG4-related kidney disease. Clin Exp Nephrol 2011;15:615-26.

[3] Yamaguchi Y, Kanetsuna Y, Honda K, Yamanaka N, Kawano M, Nagata M; Japanese study group on IgG4-related nephropathy. Characteristic tubulointerstitial nephritis in IgG4-related disease. Hum Pathol 2012;43:536-49.

[4] Raissian Y, Nasr SH, Larsen CP, Colvin RB, Smyrk TC, Takahashi N, et al. Diagnosis of IgG4-related tubulointerstitial nephritis. J Am Soc Nephrol 2011;22:1343-52.

[5] Yoshita K, Kawano M, Mizushima I, Hara S, Ito Y, Imai N, et al. Light-microscopic characteristics of IgG4-related tubulointerstitial nephritis: distinction from non-IgG4-related tubulointerstitial nephritis. Nephrol Dial Transplant 2012;27:2755-61.

[6] Umehara H, Okazaki K, Masaki Y, Kawano M, Yamamoto M, Saeki T, et al. Comprehensive diagnostic criteria for IgG4-related disease (IgG4-RD), 2011. Mod Rheumatol 2012;22:21-30.

[7] Fujii M, Sato Y, Ohara N, Hashimoto K, Kobasji H, Koyama Y, et al. Systemic IgG4-related disease with extensive peripheral nerve involvement that progressed from localized IgG4-related lymphadenopathy: an autopsy case. Diagn Pathol 2014;9:41. Doi: 10.1186/1746-1596-9-41.

[8] Senba Y, Mise K, Sumida K, Hayami N, Suwabe T, Ubara Y, et al. IgG4-Related Disease and Malignant Tumor. In: Umehara H, Okazaki K, Stone JH, Kawa S, Kawano M, editors. IgG4-Related Disease, Japan: Springer; 2014, p. 219-24.

[9] Deshpande V, Zen Y, Chan JK, Yi EE, Sato Y, Yoshino T, et al. Consensus statement on the pathology of IgG4-related disease. Mod Pathol 2012;25:1181-92.

[10] Kasashima S, Zen Y. IgG4-related inflammatory abdominal aortic aneurysm. Curr Opin Rheumatol 2011;23:18-23.

[11] Kasashima S, Zen Y, Kawashima A, Endo M, Matsumoto Y, Kasashima F. A new clinicopathological entity of IgG4-related inflammatory abdominal aortic aneurysm. J Vasc Surg 2009;49:1264-71.

[12] Tanigawa J, Daimon M, Murai M, Katsumata T, Tsuji M, Ishizaka N. Immunoglobulin G4-related coronary periarteritis in a patient presenting with myocardial ischemia. Hum Pathol 2012;43:1131-4.

[13] Guo Y, Ansdell D, Brouha S, Yen A. Coronary periarteritis in a patent with multi-organ IgG4-related disease. J Radiol Case Rep 2015;9:1-17.

[14] Kadler KE, Baldock C, Bella J, Boot-Handford RP. Collagens at a glance. J Cell Sci 2007;120:1955-8.

[15] Zeisberg M, Neilson EG. Mechanism of tubulointerstitial fibrosis. J Am Soc Nephrol 2010;21:1819-34.

[16] Kawamura R, Hisano S, Nakashima H, Takeshita M, Saito T. Immunohistological analysis for immunological response and mechanism of interstitial fibrosis in IgG4-related kidney disease. Mod Rheumatol 2015;25:571-8.

[17] Della-Torre E, Feeney E, Deshpande V, Mattoo H, Mahajan V, Kulikova M, et al. B-cell depletion attenuates serological biomarkers of fibrosis and myofibroblast activation in IgG4-related disease. Ann Rheum Dis 2015;74:2236-43.

[18] Mak KM, Chu E, Lau KH, Kwong AJ. Liver fibrosis in elderly cadavers: localization of collagen types I, III, and IV, α-smooth muscle actin, and elastic fibers. Ant Rec (Hoboken) 2012;295:1159-67.

[19] Yang J, Liu Y. Blockage of tubular epithelial to myofibroblast transition by hepatocyte growth factor prevents renal interstitial fibrosis. J Am Soc Nephrol 2002;13:96-107.

[20] Asada N, Takase M, Nakamura J, Oguchi A, Asada M, Suzuki N, et al. Dysfunction of fibroblasts of extrarenal origin underlies renal fibrosis and renal anemia in mice. J Clin Invest 2011;121:3981-90.

[21] Falke LL, Gholizadeh S, Goldschmeding R, Kok RJ, Nguyen TQ. Diverse origins of the myofibroblast — implications for kidney fibrosis. Nat Rev Nephrol 2015;11:233-44.

[22] Nakashima H, Miyake K, Moriyama M, Tanaka A, Watanabe M, Abe Y, et al. An amplification of IL-10 and TGF-beta in patients with IgG4-related tubulointerstitial nephritis. Clin Nephrol 2010;73:385-91.

[23] Fukui M, Ogawa Y, Shimmura S, Hatou S, Ichihashi Y, Yaguchi S, et al. Possible involvement of epithelial-mesenchymal transition in fibrosis associated with IgG4-related Mikulicz's disease. Mod Rheumatol 2015;25:737-43.

[24] Yamamoto M, Shimizu Y, Takahashi H, Yajima H, Yokoyama Y, Ishigami K, et al. CCAAT/enhancer binding protein α(C/EBPα)+ M2 macrophages contribute to fibrosis in IgG4-related disease ? Mod Rheumatol 2014;25:484-6.

[25] Furukawa S, Moriyama M, Tanaka A, Maehara T, Tsuboi H, Iizuka M, et al. Preferential M2 macrophages contribute to fibrosis in IgG4-related dacryoadenitis and sialoadenitis, so-called Mikulicz's disease. Clin Immunol 2015;156:9-18.

[26] Takeuchi M, Sato Y, Ohno K, Tanaka S, Takata K, Gion Y, et al. T helper 2 and regulatory T-cell cytokine production by mast cells: a key factor in the pathogenesis of IgG4-related disease. Mod Pathol 2014;27:1126-36.

[27] Stone JH, Zen Y, Deshpande V. IgG4-related disease. N Engl J Med 2012;366:539-51.

[28] Zen Y, Fujii T, Harada K, Kawano M, Yamada K, Takahira M, et al. Th2 and regulatory immune reactions are increased in immunoglobulin G4-related sclerosing pancreatitis and cholangitis. Hepatology 2007;45:1538-46.

Figure Legends

Fig. 1 Histopathological findings of IgG4-related kidney disease in autopsy cases. **A**: Storiform fibrosis (bird's-eye pattern fibrosis). Infiltrating lymphoplasmacytes are encircled by periodic-acid methenamine silver (PAM)-strong positive thick fibers (Case no. 5, PAM staining, original magnification×200). **B**: Immunostaining for IgG4. Dense IgG4-positive cells infiltrate in the interstitium (Case no. 5, original magnification×400). **C** and **D**: Fiber-rich interstitial lesions are observed around arcuate and interlobular artery (Case no. 2, PAM staining, original magnifications C, ×3; D, ×25). **E** and **F**: Fiber-rich interstitial lesions are also observed around arcuate vein (Case no. 4, PAM staining, original magnifications E, ×12.5; F, ×25). **G** and **H**: Acellular fibrous lesion with clear demarcation is observed in intracapsule and subcapsule (Case no. 1, Masson's Trichrome staining, original magnifications: G, ×3; H, ×25).

Fig. 2 Immunostaining for interstitial inflammation and fibrosis of intracapsular, subcapsular, and perineural lesions in IgG4-related kidney disease patients. Depicted stages and locations were as follows: intracapsular lesions, stage D (Case no. 1); subcapsular lesions, stage D (Case no. 1); perineural lesions, stage B (Case no. 3). Collagen I and fibronectin were dominant in intracapsular lesions. Fibronectin was

dominant in subcapsular lesions. Collagen I and III were dominant in perineural lesions. Original magnification×200.

Fig. 3 Immunostaining for interstitial inflammation and fibrosis of perivascular and cortical lesions in IgG4-related kidney disease patients. Depicted stages and locations were as follows: cortex lesions, stage A+B (Case no. 5); cortex lesions, stage C (Case no. 5); perivascular lesions, stage A+B (Case no. 1); perivascular lesions, stage D (Case no. 4). Collagen IV, VI and fibronectin were dominant in cortical lesions, including storiform fibrosis, whereas collagen I, VI and fibronectin were dominant in perivascular lesions. Original magnification×200.

Fig. 4 Alpha-smooth muscle actin (α-SMA)-positive cell infiltration according to stage. **A**: Representative images of immunostaining for α-SMA according to the stage. Original magnification×400. **B**: Comparison of α-SMA-positive cells among the stages. The number of α-SMA-positive cells decreased with increasing stage. *p <0.05. Stage A, n = 5; Stage B, n = 12; Stage C, n = 2; stage D, n = 7. 'n' means number of lesions in autopsy cases.

Table 1. Clinical and serological features of 5 autopsy cases

Case No.	Gender	Age at the time of diagnosis of IgG4-RD (years)	Period between Diagnosis of IgG4-RD and death (month)	IgG (mg/dL)	IgG4 (mg/dL)	C3 (mg/dL)	C4 (mg/dL)	CH50 (IU/mL)	Extra-renal lesions	Malignancy	CS therapy	Other therapy	Last dose of PSL (mg/dL)
1	Male	67	108	4,803	319	56	15	NA	Sa, Ao/RPF, Lu, Ly	-	+	-	5
2	Male	64	69	4,001	1,340	55	2	10	Pa	-	+	-	5
3	Male	76	1	4,813	1,750	50	2	< 15	Sa, Ao/RPF, Ec, Lu, Li, Bi, Me, Pr, Sk, Ly	-	-	-	0
4	Male	76	67	3,381	1,520	59	5	28	Pa, Sa, Lu, Ly	Lung cancer	-	Chemo	0
5	Male	73	71	2,430	1,490	90	18	45	Pa, Sa, Pr	Mucinous cyst, adenocarcinoma of the appendix	+ (past)	Chemo	0

Abbreviations: CS, corticosteroid; PSL, prednisolone; NA, not available; Sa, salivary gland; Ao/RPF, aorta and retroperitoneal fibrosis; Lu, lung; Li, liver; Ly, lymph node; Pa,

pancreas; Ec, endocrine; Bi, bile duct; Me, mesenterium; Pr, prostate; Sk, skin; Chemo, chemotherapy

Table 2. Histopathological findings of 5 autopsy cases

Case No.	IgG4-positive plasma cell infiltration (/hpf)	IgG4+/ CD138+ ratio (%)	Storiform fibrosis	Periarterial plasma cell infiltration	Periarterial fibrosis	Perivenous lesion
1	38.4	48	-	+	-	++
2	3.4	14	-	-	+++	+
3	115.8	83	+	+++	-	+++
4	80	86	-	+++	-	+++
5	77.8	110	+	+++	-	+++

Abbreviations: hpf, high power field

Table 3. Stage classification of interstitial fibrosis according to location

Case No.	Intracapsule	Subcapsule	Cortex	Perivasculature	Perinerve	Medulla
1	D	D	B	A + B	—	None
2	A	B + D	D	A + B + D	—	None
3	—	—	A + B + C	B	B	None
4	None	B	None	A + B + D	—	None
5	—	—	A + B + C	A + B	—	None

Abbreviations: -, no sample was obtained; None, no lesions existed

Table 4. Components in interstitial fibrosis according to stage and distribution

Location/Stages	Stage A	Stage B	Stage C	Stage D
Intracapsule	Negative	—	—	Col I, FN
Subcapsule	Negative	FN	—	FN
Cortex	Negative	Col IV, VI, FN	Col III, IV, VI, FN	Col III, IV, VI, FN
Perivascular	Negative	Col I, III, IV, VI, FN	—	Col I, III, VI, FN
Perinerve	Negative	Col I, III	—	—
Medulla	—	—	—	—

Abbreviations: Col, collagen; FN, fibronectin; —, no sample was obtained; Negative, no lesions existed in sample

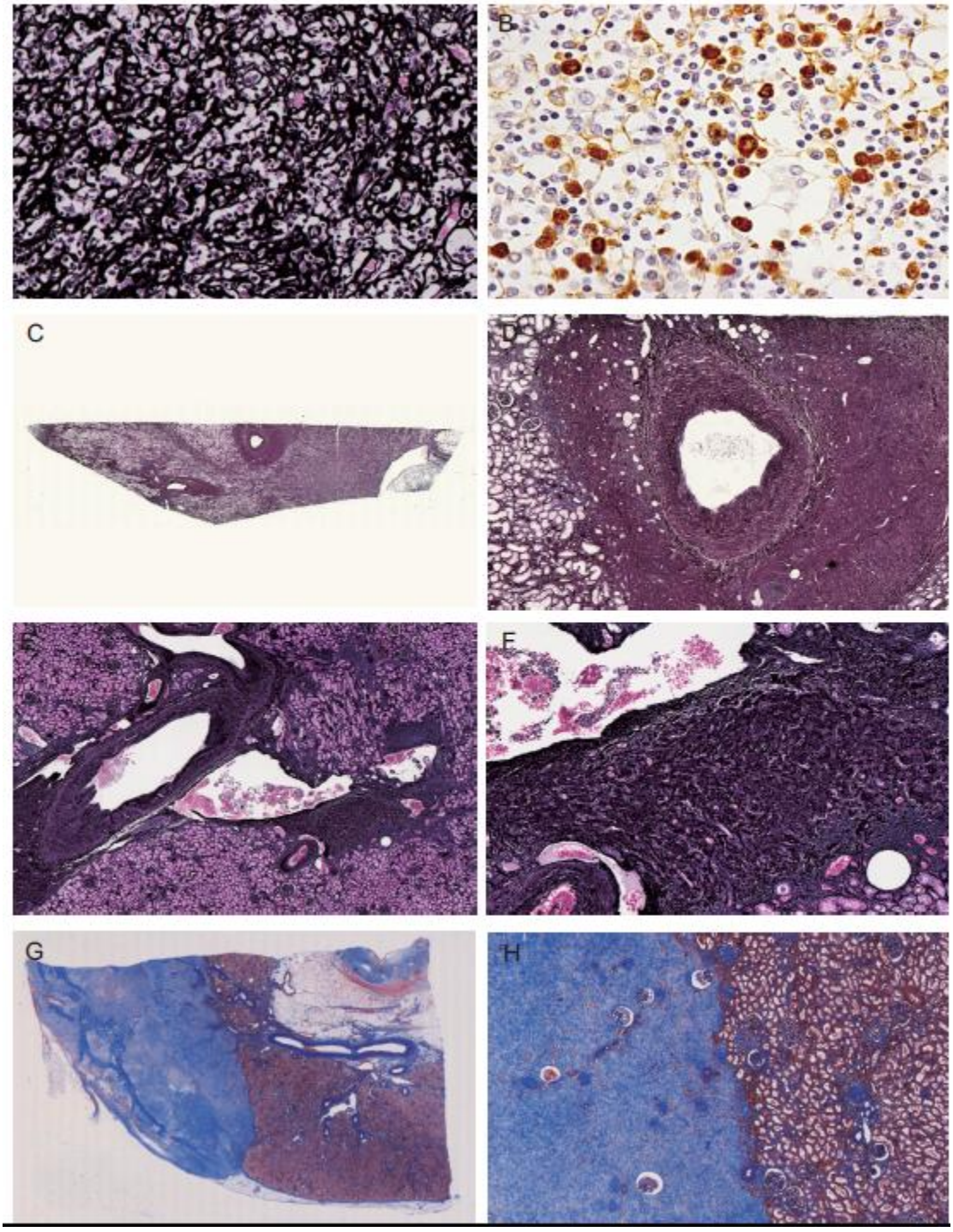

Figure 1

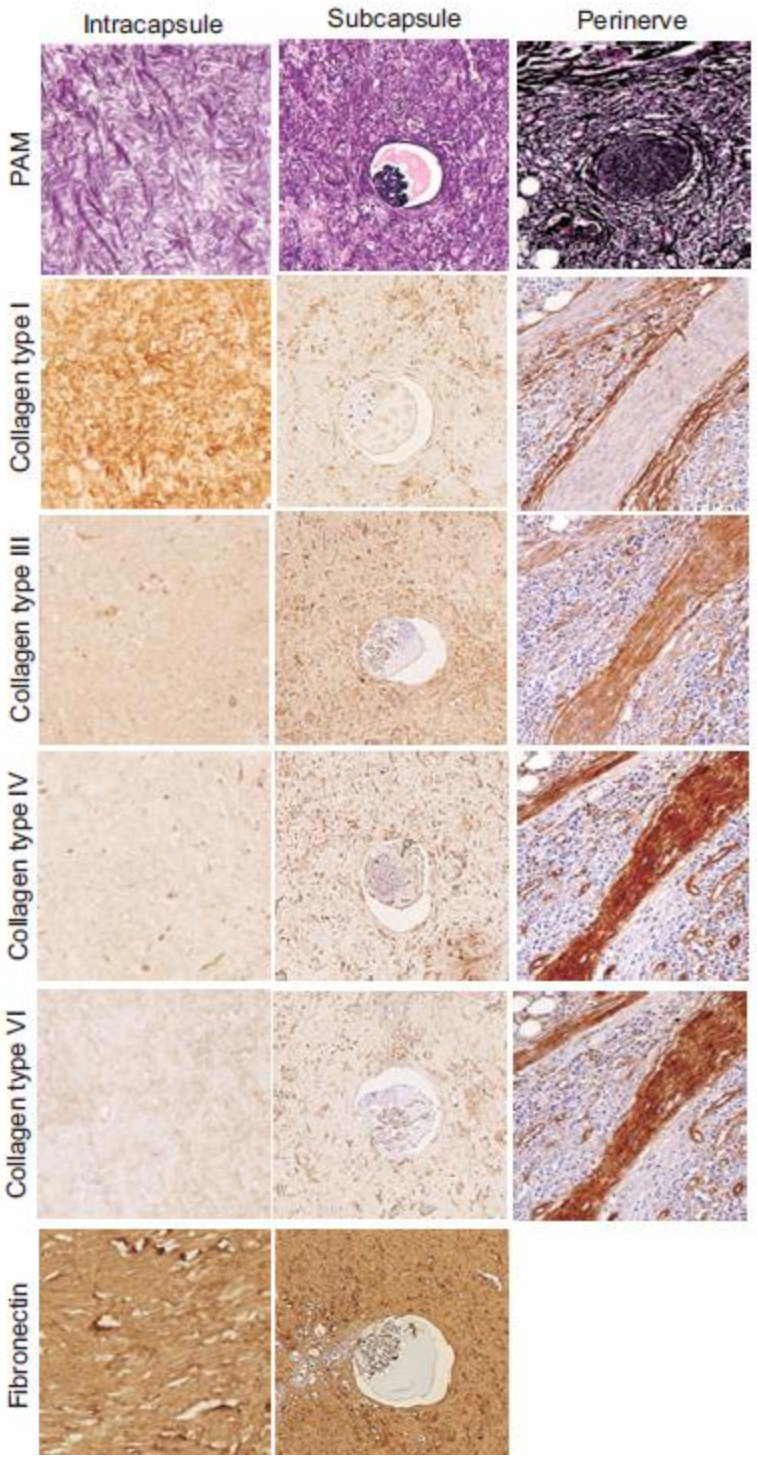

Figure 2

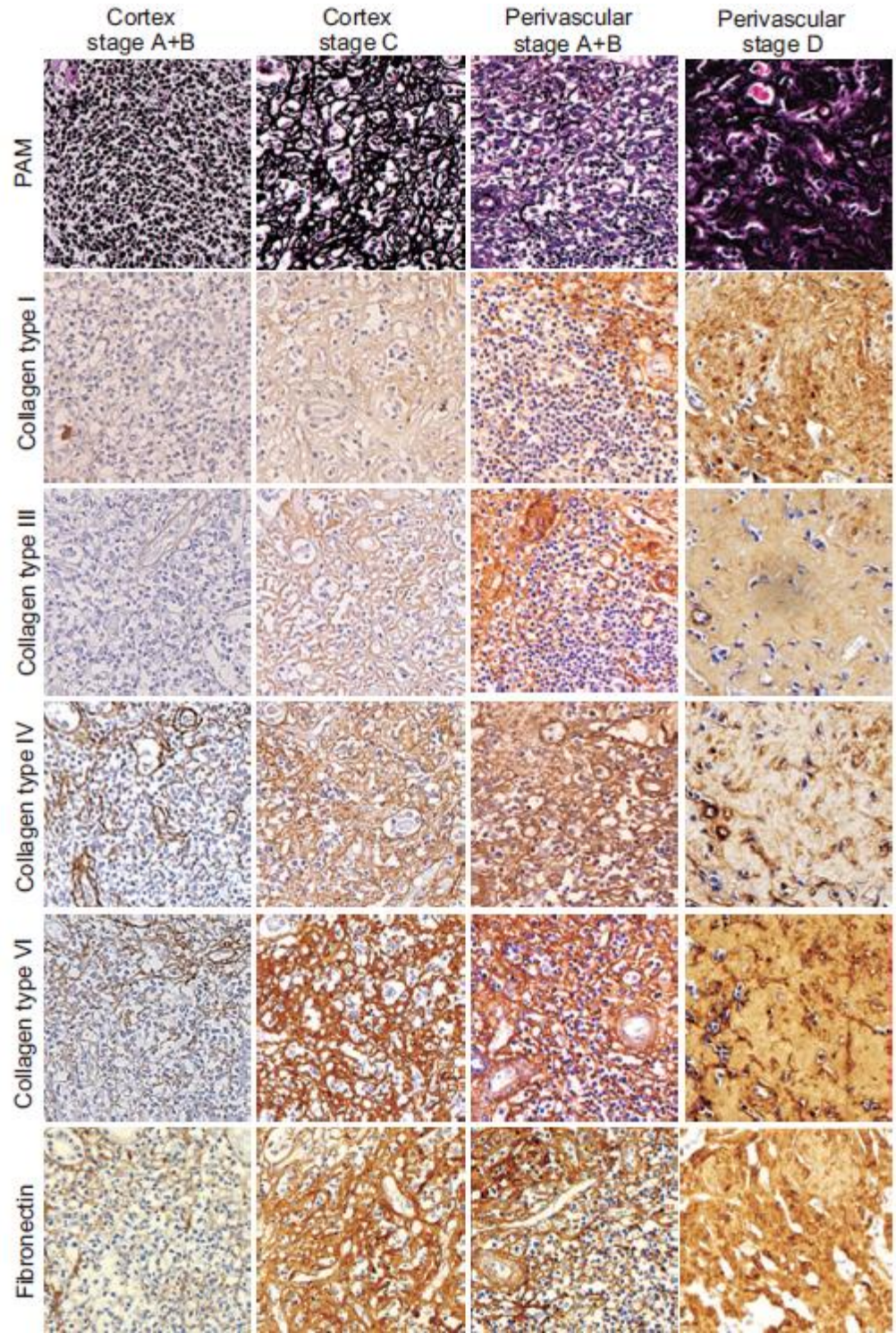

Figure 3

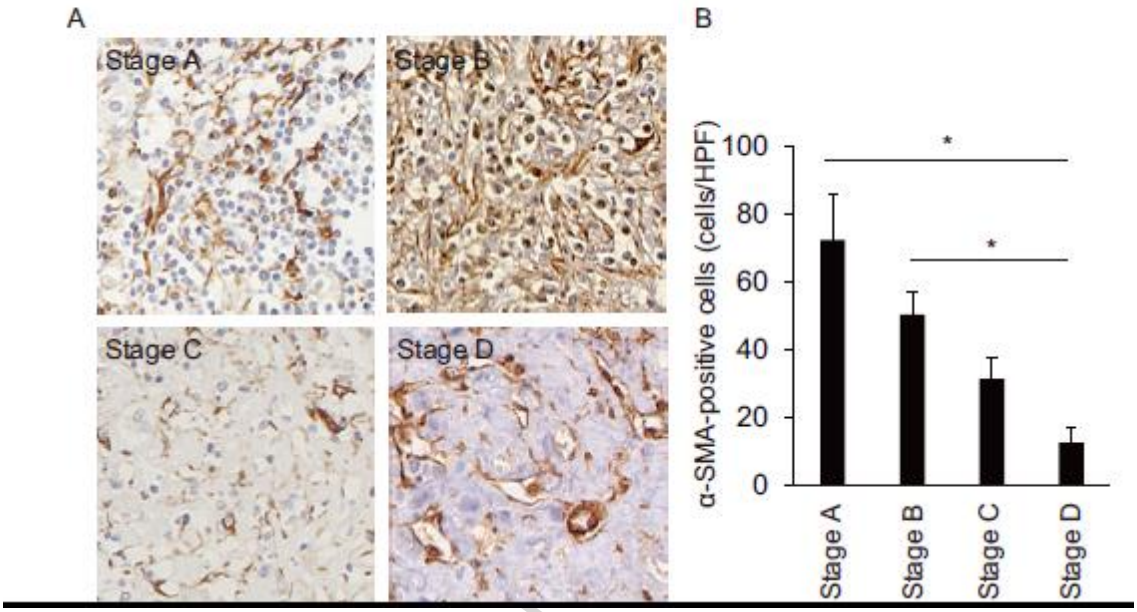

Figure 4